Vibrational Spectral Diffusion of Azide in Water†

Shuzhou Li, J. R. Schmidt, A. Piryatinski, C. P. Lawrence, and J. L. Skinner*

Theoretical Chemistry Institute and Department of Chemistry, University of Wisconsin, Madison, Wisconsin 53706

Received: December 29, 2005; In Final Form: April 27, 2006

Vibrational spectral diffusion denotes the time-dependent fluctuations of a solute's vibrational frequencies due to local environmental dynamics. Vibrational line shapes are weakly sensitive to spectral diffusion, whereas three-pulse vibrational echoes are much more sensitive. We report here on theoretical studies of spectral diffusion of the asymmetric stretch of the azide anion in heavy water. We run a classical molecular dynamics simulation of rigid azide in rigid water, and at every time step we calculate the azide's anharmonic asymmetric stretch frequency using an optimized quantum mechanics/molecular mechanics method developed earlier. This generates a frequency trajectory, which we use to calculate the absorption line shape and integrated three-pulse echo intensity. Our results for both the line width and the integrated echo intensity are in excellent agreement with experiment. Our calculated frequency time-correlation function is in excellent agreement with experiment for long times (greater than 250 fs) but differs considerably from experiment at short times; our theoretical correlation function has a very pronounced oscillation, presumably due to intermolecular azide−water hydrogen-bond stretching dynamics.

1. Introduction

Many chemical and biochemical reactions occur in the condensed phase, and the structure and dynamics of local solvation environments can be of crucial importance in determining reaction rates and pathways. A molecule's vibrational frequencies are very sensitive to its solvation environment, so as the environment evolves in time (because of molecular dynamics) the vibrational frequencies fluctuate accordingly. Such a process, known as vibrational spectral diffusion, is thus an excellent probe of solvation dynamics. With the advent of ultrafast laser techniques such as the three-pulse vibrational echo, information about vibrational spectral diffusion in the subpicosecond time range has become available.[1−20] Molecular-level interpretation of these experimental spectroscopic measurements requires a detailed understanding of the intricate relationship between the local environment and the instantaneous absorption frequency of the solute molecule's vibrations.

The triatomic azide anion, N_3^-, is especially sensitive to its surrounding solvation environment, and has been used extensively as a molecular probe to study structure and dynamics in aqueous solutions, reverse micelles, glasses, and proteins.[1,18,19,21−36] The first femtosecond three-pulse photon-echo experiment of a vibrational transition was carried out by Hamm, Lim, and Hochstrasser on the aqueous azide system.[1] In this work, the asymmetric stretch of the azide anion functions as a probe of the dynamics of the solvent, which in this case is actually D_2O. Because the instantaneous solute−solvent interactions stabilize azide resonance structures with triple-bond character,[37] the solvent molecules induce a blue shift (in this case of 56 cm^{-1}) relative to the gas phase for this vibrational mode.[1] The full width at half-maximum (fwhm) of its absorption spectrum is 18 cm^{-1}, and its first excited state lifetime is 2.3 ps.[1,18,21] The vibrational frequency time-correlation function (FTCF), which is obtained from the integrated three-pulse photon-echo intensity, decays biexponentially on time scales of approximately 80 fs and 1.3 ps.[1]

It is of interest to obtain a molecular-level understanding of these experimental results, and indeed the azide/water system is amenable to such a theoretical study.[37−40] The principle challenge is to establish a connection between the instantaneous solvation environment and the azide vibrational frequency. In a previous paper,[41] we have explored several such approaches for the calculation of vibrational frequencies, in clusters consisting of a single azide anion and its first solvation shell. These frequencies were then compared to high-level ab initio benchmark calculations on the same clusters.[41] The frequencies obtained from traditional system−bath coupling methods or from an electrostatic electronic structure approach were not in particularly good agreement with the benchmark frequencies, while extended system-bath coupling[39] and empirical frequency correlation[42,43] methods worked somewhat better. The best results came from an optimized quantum mechanical/molecular mechanical (OQM/MM) method and were in excellent agreement with the benchmark frequencies.[41]

In this paper, we apply our OQM/MM method for azide in liquid water. We first describe the azide−water intermolecular potential that was used in the molecular dynamics (MD) simulations. We then briefly describe the OQM/MM method that was used for the calculation of the asymmetric stretch vibrational frequency at every time step. This leads to a frequency trajectory, which we use to calculate results for the absorption spectrum, FTCF, and integrated photon-echo intensity. We find that our linear spectrum is in excellent agreement with experiment[18,21] for the width but in rather poor agreement for the shift. Our calculated integrated photon-echo intensity is in excellent agreement with the corresponding experimental measurements.[1] Our calculated FTCF is in excellent agreement at long times (greater than 250 fs) with the FTCF obtained from the echo data,[1] but differs considerably from experiment at short

† Part of the special issue "Robert J. Silbey Festschrift".

* Corresponding author. E-mail: skinner@chem.wisc.edu.

10.1021/jp057568k CCC: $33.50 © 2006 American Chemical Society
Published on Web 05/26/2006

TABLE 1: Positions of the First Peaks (in Å) of the Terminal Nitrogen−Deuterium (N_t−D), Terminal Nitrogen−Oxygen (N_t−O), Middle Nitrogen−Deuterium (N_m−D), and Middle Nitrogen−Oxygen (N_m−O) Radial Distribution Functions for Various Azide−Water MD Simulations

	N_t−D	N_t−O	N_m−D	N_m−O
Ferrario et al.[38]	1.70	2.69	2.54	3.44
this work	1.89	2.87	2.72	3.59
CPMD[40]	1.9	2.86	2.6	3.5

times. In particular, at short times the theoretical FTCF has a pronounced oscillation, even going slightly negative, while the experimentally derived FTCF decays monotonically. The oscillation in the theoretical FTCF presumably arises from intermolecular azide−water hydrogen-bond stretching dynamics.

II. Theoretical Methods

A. Intermolecular Potential. Modeling the dynamics of azide in water requires an accurate intermolecular potential to capture the strong interactions between the charged azide anion and the surrounding water molecules. Two research groups have carried out classical molecular dynamics (MD) simulations of azide in water.[38,39] Ferrario, Klein, and McDonald[38] considered rigid azide in (rigid) SPC/E water;[44] the azide bond lengths were 1.2 Å, the charge on each terminal nitrogen was set to −0.952 e, and the LJ parameters between nitrogen and oxygen atoms were $\sigma_{NO} = 3.243$ Å and $\epsilon_{NO}/k = 57.8$ K. They studied the reorientation time of N_3^- and obtained good agreement with experiment.[21] Morita and Kato[39] studied the vibrational relaxation of the azide asymmetric stretch using a similar model; the charge on each terminal nitrogen was reduced to −0.9215 e, the bond lengths were 1.1626 Å, and they used a flexible SPC model.

Yarne, Tuckerman, and Klein have also previously examined the structural and dynamical behavior of a single azide anion in water from Car−Parrinello molecular dynamics (CPMD) calculations.[40] Because CPMD does not make any assumptions regarding the intermolecular potential, it can serve as a reference against which to evaluate empirical potentials when experimental measurements are not present.[45] We compared results of the model used by Ferrario et al.[38] with the CPMD results and found some disagreement in that the first peak of the O−N_t (N_t denotes terminal nitrogen) radial distribution function from the classical MD simulation is about 0.2 Å closer than that from CPMD (see Table 1).

Because of the above discrepancy, we set out to modify the model of Ferrario et al. The azide geometry was taken from a gas-phase ab initio calculation; at the B3LYP level with a 6-311++G(d,p) basis set, the azide is linear, and the optimized bond lengths are 1.1833 Å, which is in excellent agreement with the experimentally measured bond length of 1.1884 Å.[46] The charge assigned to each terminal nitrogen atom is −0.9531 e, which comes from a CHelpG analysis.[47] To reproduce the CPMD radial distribution functions, we increased σ_{NO} to 3.403 Å (ϵ_{NO} was kept unchanged). The resulting radial distribution functions (see below for simulation details) are shown in Figure 1, and the first peak positions are summarized and compared with the corresponding CPMD results in Table 1. The radial distribution functions from the new simulations are in reasonable agreement with those from CPMD. The average number of water molecules in the first solvation shell, determined by integrating the O−N_t distribution function up to the first minimum, is between five and six in the CPMD simulations, and between six and seven in our classical MD simulations.

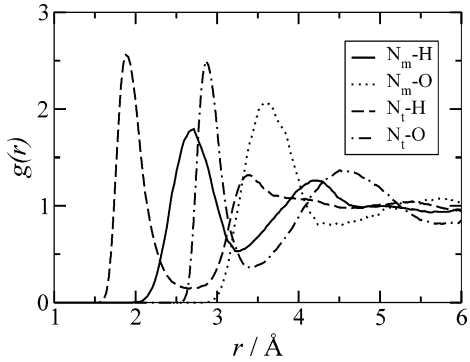

Figure 1. Azide−water radial distribution functions. N_m and N_t denote middle and terminal nitrogen atoms, respectively.

B. MD Simulations. The simulation system consisted of 107 rigid (SPC/E) D_2O molecules and one rigid azide ion. Cubic periodic boundary conditions were applied, and the size of the box was chosen such that the molecular density, including the one azide ion, is the same as the experimental value for D_2O at 300 K, which is 3.32×10^{28} m^{-3}.[48] The electrostatic forces were calculated using an approximation to the Ewald sum, as described by Adams and Dubey.[49] The equations of motion were integrated using the leapfrog algorithm with a time step of 1 fs, and the rotational degrees of freedom were treated using quaternions. The system was first equilibrated by periodically rescaling the velocities of the molecules. This continued until the temperature reached the desired value of 300 K and was maintained to within ±1 K for 80 ps without adjustment. The production runs, from which all subsequent results were derived, were at least 1 ns long.

C. OQM/MM Method for Calculating Vibrational Frequencies. In a previous paper, we developed the OQM/MM method for the calculation of vibrational frequencies in solution.[41] The QM/MM parameters were optimized by comparing computed frequencies for azide/water clusters to those from reasonably accurate density functional theory calculations. The method reproduces the ab initio frequencies for 50 representative N_3^-/D_2O clusters with an RMS deviation of 7.2 cm^{-1}.[41] Here we apply this OQM/MM method to the liquid phase without any further modification. The method is summarized briefly below, and complete details are given elsewhere.[41]

We treat the azide anion with the semiempirical PM3 Hamiltonian,[50] while the remaining solvent molecules are treated in the SPC/E water model MM representation. QM/MM interactions are accounted for by letting the MM point charges polarize the QM wave function and incorporating core−core repulsion between the QM nuclei and the MM point charges, in both cases as described by Field et al.[51] All QM/MM calculations were carried out using a modified version of the MOPAC 7 package, which was extended to incorporate QM/MM interactions.

At each simulation time step we calculate the anharmonic azide asymmetric stretch vibrational frequency according to the following algorithm:[41] we first optimize the bond lengths of the azide, subject to the constraints that the azide center of mass and orientation remain fixed. The potential energy curves for each of the two independent N−N local mode coordinates, denoted x and y, were then calculated by scanning each of these coordinates individually while holding the other (and the center of mass and orientation) fixed. The curves were fit to a Morse form, and the bilinear coupling term, k_{xy}, was evaluated by a numerical second derivative about the potential minimum. The vibrational eigenstates of the resulting Hamiltonian were

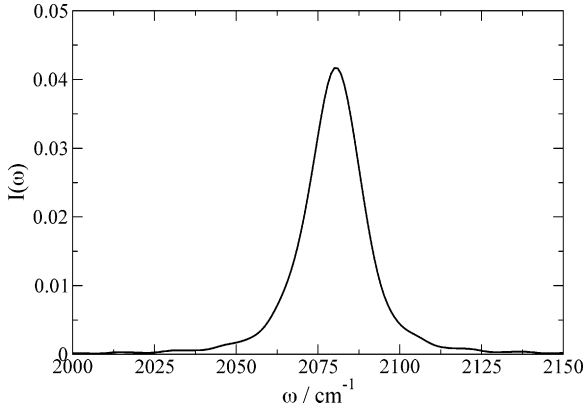

Figure 2. Calculated absorption spectrum for the azide asymmetric stretch.

TABLE 2: Shift and Width Values (in cm^{-1}) for OQM/MM and Experimental Line Shapes

	$\langle\omega\rangle$	FWHM
QM/MM	94	18.8
experiment[21]	56.5	20
experiment[18]	56.0	17.8

calculated to yield the asymmetric stretch frequency. The OQM/MM method was applied at each MD simulation time step to calculate this frequency, resulting in a frequency trajectory that was used in the subsequent analysis.

III. Results and Discussion

A. Absorption Line Shape. For the purposes of computing the infrared spectrum within a classical MD simulation, it is appropriate to begin with a semiclassical approximation to the absorption line shape:[42,52−58]

$$I(\omega) \sim \int_{-\infty}^{\infty} \mathrm{d}t\, \mathrm{e}^{-i(\omega - \langle\omega\rangle)t} \langle \exp[-i \int_0^t \mathrm{d}\tau \delta\omega(\tau)] \rangle \mathrm{e}^{-|t|/2T_1} \quad (1)$$

In the above expression, $\langle\omega\rangle$ is the average absorption frequency for the vibrational mode of interest, $\delta\omega(\tau) = \omega(\tau) - \langle\omega\rangle$ is the time-dependent frequency fluctuation from its average value, T_1 is the lifetime of the first excited state, and the angular brackets indicate a classical equilibrium statistical mechanical average. Note that in this expression we have made the Condon approximation and have neglected the effects of rotations. For N_3^- in D_2O, the experimental lifetime of the first excited state of the asymmetric stretch is 2.3 ps,[1,21] which was used in this and subsequent calculations. The frequency is written as[41] $\omega = \omega_0 + \Delta\omega$, where ω_0 is the gas-phase frequency (from either experiment or theory because the latter is scaled by 0.975 to obtain the former[41]) and $\Delta\omega$ is the perturbation due to the solvent. The frequency trajectory from the OQM/MM approach was used to calculate the line shape, which, as shown in Figure 2, is completely structureless, and can therefore be well-characterized by the solvent shift $\langle\Delta\omega\rangle$ and fwhm, which are summarized in Table 2.

Two research groups have measured the experimental absorption line shape of this system, and the results from each group are also given in Table 2.[18,21] The fwhm of the absorption spectrum measured by the Hochstrasser group is 20 cm^{-1}, while a more recent measurement by the Tominaga group yielded 17.8 cm^{-1}. Our OQM/MM result of 18.8 cm^{-1} agrees very nicely with this range. The theoretical fwhm of the frequency distribution is 51 cm^{-1}, which is much larger than the fwhm of the absorption line shape, indicating substantial motional narrowing. Our computed frequency shift of 94 cm^{-1} is quite a bit larger than the experimental measurement of 56 cm^{-1}.[18,21]

The accuracy of the computed solvent shift depends on the following: (1) the accuracy to which we can calculate the vibrational frequency for a given solvent configuration and (2) the extent to which the solvent configurations from the simulations mimic reality. Given our studies on azide/water clusters, we are reasonably confident about the former,[41] implying that the source of the discrepancy must come from the latter, which in turn indicates a deficiency in the intermolecular azide−water potential used in the simulation. Any deficiencies in this potential would bias the sampling of solute−solvent configurations, and therefore bias the resulting vibrational frequencies. For example, the coordination number in the CPMD simulations[40] is between five and six, whereas our MD simulations yield between six and seven. Thus, it is likely that the classical MD simulation includes too many water molecules in the azide first solvation shell, resulting in an overestimation of the blue shift. Additionally, the azide solvochromic shift is extremely sensitive to the distance of closest azide−water approach; if the repulsive wall of the potential is too weak, then the average frequency shift would be biased to the blue. Further study is needed to resolve fully this issue.

B. Integrated Three-Pulse Photon Echo. As is well known, it is difficult to obtain information about spectral diffusion from line shapes. In contrast, the three-pulse photon-echo experiment is designed to provide a reasonably direct probe of these dynamics. Hochstrasser and co-workers performed an integrated three-pulse echo experiment on the asymmetric stretch of azide in heavy water.[1]

The three-pulse echo is generated from a sequence of three pulses with specific wavevectors. The time delay between pulses 1 and 2 is t_1, that between the later of pulses 1 and 2 and pulse 3 is t_2, and the time after pulse 3 is t_3. In the integrated three-pulse echo experiment, one measures the intensity of the photon-echo signal, integrated over t_3, as a function of t_1 and t_2. In the impulsive limit, where the length of the pulses are short compared to all other relevant time scales in the problem, the integrated echo intensity is given by

$$I(t_2, t_1) = \begin{cases} \int_0^{\infty} \mathrm{d}t_3 \left|\sum_{i=1}^{3} R_i(t_3, t_2, t_1)\right|^2, & \text{if } t_1 > 0, \\ \int_0^{\infty} \mathrm{d}t_3 \left|\sum_{i=4}^{6} R_i(t_3, t_2, t_1)\right|^2, & \text{if } t_1 < 0 \end{cases} \quad (2)$$

In the above, $R_i(t_3, t_2, t_1)$ are the nonlinear response functions.[1,55,59,60] These expressions can be generalized to account for finite pulse duration, in which case two additional response functions are needed, and the response functions must be convoluted over the electric fields of the three laser pulses.[55] Because preliminary calculations[61] show that both the cumulant and Condon approximations work reasonably well for the azide/water system, we will use the well-known cumulant approximations to R_i.[1,55,59,60] Vibrational relaxation was accounted for as described by Hamm et al.[1] using the experimentally measured values for the lifetimes of both the first and second excited states.[1] The response functions were convoluted over 120 fs Gaussian pulses to allow for comparison with the results of Hamm et al.[1]

The integrated echo intensity was calculated for several values of t_2, and the results are shown alongside the corresponding experimental results[1] in Figure 3. For each t_2, the theoretical results are scaled to match the experimental intensity. In general,

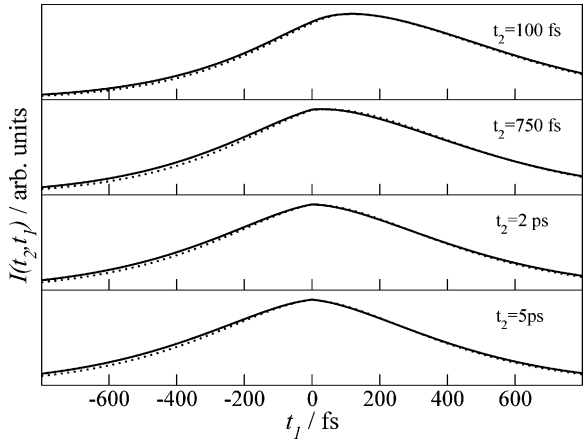

Figure 3. Calculated and experimental[1] integrated three-pulse photon-echo intensities for several delay times t_2. The theoretical OQM/MM results are shown as solid lines, and the experimental results are dotted.

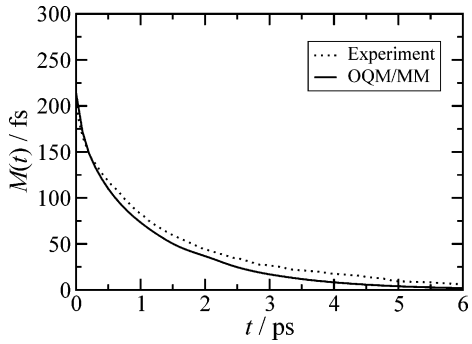

Figure 4. Calculated and experimental[1] first moment of the integrated three-pulse photon-echo intensity.

the agreement between the theoretical result and the measured echo intensity is excellent. In particular, for the earliest measured delay times of $t_2 = 100$ fs, both the theoretical and experimental results yield a peak shift of approximately 120 fs. The discrepancy between theory and experiment grows slightly for large t_2, when the integrated echo intensity becomes slightly too symmetric about $t_1 = 0$ compared with experiment. We note that the theoretical peak shift decays monotonically as a function of t_2 (starting from $t_2 = 0$).

The first moment of the integrated echo intensity is

$$M(t_2) = \frac{\int_{-\infty}^{\infty} \mathrm{d}t_1 t_1 I(t_2, t_1)}{\int_{-\infty}^{\infty} \mathrm{d}t_1 I(t_2, t_1)} \tag{3}$$

Our calculation of the first moment is plotted alongside the corresponding experimental measurement[1] in Figure 4. Note that in both cases the actual upper and lower limits of the above integrals was ± 1 ps (because data was not taken outside this range). One sees that the theoretical and experimental first moments are also in excellent agreement. The only noticeable discrepancies arise for large t_2, where the experimental first moment is distinctly nonzero. This behavior arises from a small, low-amplitude, inhomogeneous term in the experimentally derived FTCF, which presumably arises from dynamics that happen on a time scale slower than that which is experimentally resolvable. We do not see evidence for such slow dynamics in our theoretical calculation.

C. Frequency Time-Correlation Function. As discussed above, vibrational photon-echo experiments are traditionally analyzed within the nonlinear response function formalism,[55]

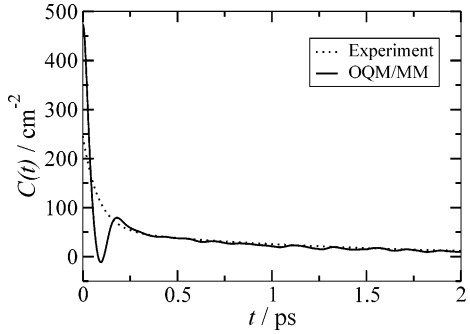

Figure 5. Calculated and experimental[1] frequency time-correlation functions.

making the cumulant and Condon approximations. In this case, the central object of interest is the equilibrium frequency time-correlation function (FTCF), defined by $C(t) = \langle \delta\omega(t)\, \delta\omega(0) \rangle$. Hamm et al. assumed that the FTCF could be described by a sum of two decaying exponentials plus a constant term.[1] Performing a global fit of their photon-echo data, they obtained a result for the FTCF shown in Figure 5. From our frequency trajectory, we also calculated the FTCF, and our results are shown in Figure 5. One sees that after about 250 fs the theoretical and experimental FTCFs are virtually identical, whereas for times less than 250 fs they are quite different. In particular, the initial value of the theoretical FTCF is nearly twice as large as that from experiment, the theoretical FTCF decays substantially faster, and the theoretical FTCF shows a very pronounced oscillation with a period of around 180 fs and small recurrences of the oscillation even for times greater than 1 ps.

It is important to emphasize that both theoretical and experimental FTCFs reproduce both the line shape and the three-pulse photon-echo intensity. In particular, a signature of the pronounced oscillation in the theoretical FTCF does not appear in the theoretical peak shift (see above) because of the convolutions with the finite pulses. This suggests that this experiment is not very sensitive to details of the short-time dynamics, which in turn may imply that inversion of the photon-echo data to obtain the (short-time features of the) FTCF may be problematic. Additionally, the biexponential functional form used by Hamm et al. in their inversion procedure[1] means that it would not have been possible for them to obtain the oscillatory behavior in the FTCF.

The long-time decay in the FTCF was originally interpreted by Hamm et al. as arising from the making and breaking of azide−water hydrogen bonds.[1] For the related HOD/D_2O system, the decay of the OH-stretch FTCF was similarly associated with hydrogen-bond dynamics.[62−66] To test this interpretation, we studied the hydrogen-bond dynamics of the azide/water system. Because there is no clear definition of the azide−water hydrogen bond, we simply chose to define all waters with deuterium atoms whose distances from either terminal nitrogen were smaller than 2.7 Å (the first minimum of the N_t−D radial distribution function) to be hydrogen bonded with the azide anion. Using this definition, we calculated the hydrogen bond number fluctuation TCF $\langle \delta n(t)\, \delta n(0) \rangle$, where $\delta n(t) = n(t) - \langle n \rangle$ is the fluctuation of the number of hydrogen bonds from equilibrium. The resulting normalized hydrogen-bond TCF is plotted in Figure 6. Also shown in the plot is the normalized FTCF. In the logarithmic plot (lower panel), the hydrogen-bond TCF decays slightly faster at long time than the FTCF. Several alternative hydrogen-bond definitions all yielded similar long-time decays.

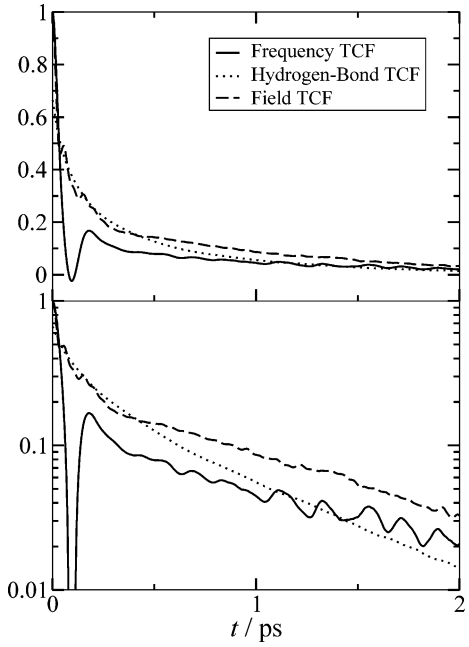

Figure 6. Normalized frequency, hydrogen-bond, and electric field time-correlation functions. The lower panel shows a log plot.

The slower time scale of the FTCF at long times suggests that some more collective dynamics may be influencing the azide frequency fluctuations.[67] For the azide system especially, because the azide is charged, it would be expected to have longer-ranged interactions, and so be more sensitive to collective fluctuations. To this end, we calculated the projection of the electric field along the molecular axis, due to the surrounding SPC/E water molecules, at the two terminal nitrogens. Letting the difference in these fields be E, we calculated the field TCF $\langle \delta E(t)\ \delta E(0)\rangle$, where $\delta E(t) = E(t) - \langle E\rangle$. The resulting normalized TCF is plotted in Figure 6. The decay of the field TCF is very similar to that of the FTCF at long times, which is consistent with recent findings of Eaves et al. for the HOD/D_2O system.[67] Note, however, that these two viewpoints (hydrogen bond versus electric field fluctuations) are not really mutually exclusive because the field itself is dominated by the nearest neighbors, the ones involved in making and breaking hydrogen bonds.

To understand the short-time oscillation in the theoretical FTCF, we obtained the N_t-O potential of mean force from the N_t-O radial distribution function, and fit the first minimum to a parabolic form to give the characteristic force constant corresponding to the azide−water intermolecular vibration. Using the reduced mass for the ion−molecule pair, the period was calculated to be 200 fs. A similar calculation from the N_t-D distribution function yielded 190 fs. Both of these times are in rough agreement with the observed FTCF oscillation period of around 180 fs, and thus we conclude that the (underdamped) intermolecular azide−water hydrogen-bond stretch produces this oscillation.

IV. Concluding Remarks

As demonstrated by our previous study of azide/water clusters,[41] the aqueous azide system presents a formidable computational challenge for the calculation of condensed-phase vibrational spectroscopy. Using the OQM/MM method, we have calculated the azide linear spectrum, FTCF, and the integrated three-pulse photon-echo signal. Our confidence in the method is bolstered by the excellent agreement between theory and experiment for the line width and the echo intensity. However, our calculated value of the solvent shift is substantially too large. We believe that this is due to inaccuracies in the azide−water intermolecular potential surface. This emphasizes the point that even if we can calculate accurate vibrational frequencies our results for observables may be poor if the intermolecular interaction potential surface is inadequate. Nonetheless, we believe that the OQM/MM method represents a flexible, accurate, and general approach to vibrational spectroscopy in liquid-state systems.

It is interesting to contrast azide in D_2O with the HOD/D_2O system. The FTCF for the latter was determined by three-pulse photon-echo experiments by Tokmakoff and co-workers.[7,11] They found a pronounced oscillation in their FTCF, which again was attributed[7] to the intermolecular hydrogen-bonding stretching motion.[62,63,65] The water system appears to be more complicated than aqueous azide in the sense that the cumulant and Condon approximations do not hold as well for water.[59,68,69] The former is easy to understand in that for the OH stretch of HOD there is at most one hydrogen bond that strongly influences the frequency, whereas for azide there are five or six. Moreover, because azide is charged, its intermolecular interactions are longer ranged. Both of these features suggest that the central limit theorem would apply better for azide, which is one route to Gaussian statistics. Because of the (at least partial) nonelectrostatic origin of hydrogen bonding in water,[70] the vibrational transition dipole moment is strongly dependent on its local environment,[71] which is a breakdown of the Condon approximation. Therefore, it is not necessarily straightforward to "invert" photon-echo data for water to obtain the FTCF, and we think it is likely that to some extent the observed oscillation[7] is a result of this problematic inversion procedure.[59] Simulated FTCFs for water can also show a small oscillation, depending on the water model.[7,62,63,65,72] A possible explanation for the difference in the strength of the oscillation for the water and aqueous azide systems (at least from theory) is suggested from a comparison of the hydrogen-bond TCF for HOD in D_2O[62] with the corresponding quantity for the azide/water system shown in Figure 6. From these figures it is evident that, for times less than 200 fs, the azide loses much less of its hydrogen-bond number correlation than HOD, perhaps because of the stronger electrostatic azide−water interaction. If the vibrations of the intermolecular azide−water hydrogen bonds dominate the frequency correlation for these short times, then the relatively slower decay of the associated hydrogen-bond TCF could explain the strength of the observed oscillation in the FTCF.

We close with a brief discussion of solvent isotope effects. Experimental results show an additional 5 or 6 cm^{-1} blue shift on changing the solvent from D_2O to H_2O,[18,21] presumably from reduced vibrational coupling to the nonresonant OH stretch (compared to the OD stretch).[41] Such an effect is not accounted for in the present method because the calculated anharmonic frequencies were obtained using a procedure that does not involve intermolecular vibrational coupling between the azide and the surrounding water molecules. However, preliminary normal-mode calculations[61] on 100 azide/water clusters show that this trend can be captured, at least qualitatively, because the average frequency in the H_2O clusters is 19 cm^{-1} to the blue of that for the corresponding D_2O clusters. The lack of quantitative agreement with experiment is likely due to the harmonic approximation, the improper use of normal-mode analysis when not at a global minimum, or the previously discussed bias in the sampled clusters due to an approximate intermolecular potential.

Acknowledgment. We thank our colleague Marty Zanni for helpful discussions. We are grateful for support from the National Science Foundation, through grants CHE-0132538 and CHE-0446666, and from the Fannie and John Hertz Foundation through a fellowship to J.R.S.

References and Notes

(1) Hamm, P.; Lim, M.; Hochstrasser, R. M. *Phys. Rev. Lett.* **1998**, *81*, 5326.
(2) Asbury, J. B.; Steinel, T.; Stromberg, C.; Gaffney, K.; Piletic, I. R.; Goun, A.; Fayer, M. D. *Chem. Phys. Lett.* **2003**, *374*, 362.
(3) Khalil, M.; Demirdöven, N.; Tokmakoff, A. *J. Chem. Phys. A* **2003**, *107*, 5258.
(4) Thompson, D. E.; Merchant, K. A.; Fayer, M. D. *J. Chem. Phys.* **2001**, *115*, 317.
(5) Zanni, M. T.; Asplund, M. C.; Hochstrasser, R. M. *J. Chem. Phys.* **2001**, *114*, 4579.
(6) Hamm, P.; Lim, M.; Hochstrasser, R. M. *J. Phys. Chem. B* **1998**, *102*, 6123.
(7) Fecko, C. J.; Eaves, J. D.; Loparo, J. J.; Tokmakoff, A.; Geissler, P. L. *Science* **2003**, *301*, 1698.
(8) Asbury, J. B.; Steinel, T.; Stromberg, C.; Corcelli, S. A.; Lawrence, C. P.; Skinner, J. L.; Fayer, M. D. *J. Phys. Chem. A* **2004**, *108*, 1107.
(9) Steinel, T.; Asbury, J. B.; Corcelli, S. A.; Lawrence, C. P.; Skinner, J. L.; Fayer, M. D. *Chem. Phys. Lett.* **2004**, *386*, 295.
(10) Loparo, J. J.; Fecko, C. J.; Eaves, J. D.; Roberts, S. T.; Tokmakoff, A. *Phys. Rev. B* **2004**, *70*, 180201.
(11) Fecko, C. J.; Loparo, J. J.; Roberts, S. T.; Tokmakoff, A. *J. Chem. Phys.* **2005**, *122*, 054506.
(12) Laenen, R.; Simeonidis, K.; Laubereau, A. *J. Phys. Chem. B* **2002**, *106*, 408.
(13) Deàk, J. C.; Rhea, S. T.; Iwaki, L. K.; Dlott, D. D. *J. Phys. Chem. A* **2000**, *104*, 4866.
(14) Gallot, G.; Lascoux, N.; Gale, G. M.; Leicknam, J.-C.; Bratos, S.; Pommeret, S. *Chem. Phys. Lett.* **2001**, *341*, 535.
(15) Stenger, J.; Madsen, D.; Hamm, P.; Nibbering, E. T. J.; Elsaesser, T. *J. Phys. Chem. A* **2002**, *106*, 2341.
(16) Ohta, K.; Maekawa, H.; Saito, S.; Tominaga, K. *J. Phys. Chem. A* **2003**, *107*, 5643.
(17) Cowan, M. L.; Bruner, B. D.; Huse, N.; Dwyer, J. R.; Chugh, B.; Nibbering, E. T. J.; Elsaesser, T.; Miller, R. D. J. *Nature* **2005**, *434*, 199.
(18) Maekawa, H.; Ohta, K.; Tominaga, K. *Phys. Chem. Chem. Phys.* **2004**, *6*, 4074.
(19) Maekawa, H.; Ohta, K.; Tominaga, K. *Res. Chem. Intermed.* **2005**, *31*, 703.
(20) Eaves, J. D.; Loparo, J. J.; Fecko, C. J.; Roberts, S. T.; Tokmakoff, A.; Geissler, P. L. *Proc. Natl. Acad. Sci.* **2005**, *102*, 13019.
(21) Li, M.; Owrutsky, J.; Sarisky, M.; Culver, J. P.; Yodh, A.; Hochstrasser, R. M. *J. Chem. Phys.* **1993**, *98*, 5499.
(22) Sando, G. M.; Dahl, K.; Owrutsky, J. C. *J. Phys. Chem. A* **2004**, *108*, 11209.
(23) Zhong, Q.; Baronavski, A. P.; Owrutsky, J. C. *J. Chem. Phys.* **2003**, *118*, 7074.
(24) Owrutsky, J. C.; Kim, Y. R.; Li, M.; Sarisky, M. J.; Hochstrasser, R. M. *Chem. Phys. Lett.* **1991**, *184*, 368.
(25) Zhong, Q.; Steinhurst, D. A.; Carpenter, E. E.; Owrutsky, J. C. *Langmuir* **2002**, *18*, 7401.
(26) Zhong, Q.; Baronavski, A. P.; Owrutsky, J. C. *J. Chem. Phys.* **2003**, *119*, 9171.
(27) Zhong, Q.; Owrutsky, J. C. *Chem. Phys. Lett.* **2004**, *383*, 176.
(28) Sando, G. M.; Dahl, K.; Zhong, Q.; Owrutsky, J. C. *J. Phys. Chem. A* **2005**, *109*, 5788.
(29) Asplund, M. C.; Lim, M.; Hochstrasser, R. M. *Chem. Phys. Lett.* **2000**, *323*, 269.
(30) Yang, X.; Kiran, B.; Wang, X.-B.; Wang, L.-S.; Mucha, M.; Jungwirth, P. *J. Phys. Chem. A* **2004**, *108*, 7820.
(31) Waterland, M. R.; Kelley, A. M. *J. Phys. Chem. A* **2001**, *105*, 8385.
(32) Fulmer, E. C.; Ding, F.; Zanni, M. T. *J. Chem. Phys.* **2005**, *122*, 034302.
(33) Fulmer, E. C.; Ding, F.; Mukherjee, P.; Zanni, M. T. *Phys. Rev. Lett.* **2005**, *94*, 067402.
(34) Jonsson, B. M.; Hakansson, K.; Liljas, A. *FEBS* **1993**, *322*, 186.
(35) Teraoka, J.; Yamamoto, N.; Matsumoto, Y.; Kyogoku, Y.; Sugeta, H. *J. Am. Chem. Soc.* **1996**, *118*, 8875.
(36) Lim, M.; Hamm, P.; Hochstrasser, R. M. *Proc. Natl. Acad. Sci. U.S.A.* **1998**, *95*, 15315.
(37) Garcia-Viloca, M.; Nam, K.; Alhambra, C.; Gao, J. *J. Phys. Chem. B* **2004**, *108*, 13501.
(38) Ferrario, M.; Klein, M. L.; McDonald, I. R. *Chem. Phys. Lett.* **1993**, *213*, 537.
(39) Morita, A.; Kato, S. *J. Chem. Phys.* **1998**, *109*, 5511.
(40) Yarne, D. A.; Tuckerman, M. E.; Klein, M. L. *Chem. Phys.* **2000**, *258*, 163.
(41) Li, S.; Schmidt, J. R.; Corcelli, S. A.; Lawrence, C. P.; Skinner, J. L. *J. Chem. Phys.*, in press.
(42) Corcelli, S. A.; Lawrence, C. P.; Skinner, J. L. *J. Chem. Phys.* **2004**, *120*, 8107.
(43) Kwac, K.; Cho, M. *J. Chem. Phys.* **2003**, *119*, 2247.
(44) Berendsen, H. J. C.; Grigera, J. R.; Straatsma, T. P. *J. Phys. Chem.* **1987**, *91*, 6269.
(45) Allesch, M.; Schwegler, E.; Gygi, F.; Galli, G. *J. Chem. Phys.* **2004**, *120*, 5192.
(46) Polak, M.; Gruebele, M.; Saykally, R. J. *J. Am. Chem. Soc.* **1987**, *109*, 2884.
(47) Breneman, C. M.; Wiberg, K. B. *J. Comput. Chem.* **1990**, *3*, 361.
(48) Franks, F., Ed. *Water: A Comprehensive Treatise*; Plenum Press: New York, 1972; Vol. 1.
(49) Adams, D. J.; Dubey, G. S. *J. Comput. Phys.* **1987**, *72*, 156.
(50) Stewart, J. P. *J. Comput. Chem.* **1989**, *10*, 209.
(51) Field, M. J.; Bash, P. A.; Karplus, M. *J. Comput. Chem.* **1990**, *11*, 700.
(52) Lawrence, C. P.; Skinner, J. L. *J. Chem. Phys.* **2002**, *117*, 8847.
(53) Corcelli, S. A.; Skinner, J. L. *J. Phys. Chem. A* **2005**, *109*, 6154.
(54) Stephens, M. D.; Saven, J. G.; Skinner, J. L. *J. Chem. Phys.* **1997**, *106*, 2129.
(55) Mukamel, S. *Principles of Nonlinear Optical Spectroscopy;* Oxford: New York, 1995.
(56) Saven, J. G.; Skinner, J. L. *J. Chem. Phys.* **1993**, *99*, 4391.
(57) Fried, L. E.; Mukamel, S. *Adv. Chem. Phys.* **1993**, *84*, 435.
(58) Oxtoby, D. W.; Levesque, D.; Weis, J.-J. *J. Chem. Phys.* **1978**, *68*, 5528.
(59) Schmidt, J. R.; Corcelli, S. A.; Skinner, J. L. *J. Chem. Phys.* **2005**, *123*, 044513.
(60) Hamm, P.; Hochstrasser, R. M. In *Ultrafast Infrared and Raman Spectroscopy*; Fayer, M. D., Ed.; Markel Dekker: New York, 2001; p 273.
(61) Li, S. Unpublished work.
(62) Lawrence, C. P.; Skinner, J. L. *J. Chem. Phys.* **2003**, *118*, 264.
(63) Rey, R.; Møller, K. B.; Hynes, J. T. *J. Phys. Chem. A* **2002**, *106*, 11993.
(64) Rey, R.; Møller, K. B.; Hynes, J. T. *Chem. Rev.* **2004**, *104*, 1915.
(65) Lawrence, C. P.; Skinner, J. L. *Chem. Phys. Lett.* **2003**, *369*, 472.
(66) Laenen, R.; Rauscher, C.; Laubereau, A. *Phys. Rev. Lett.* **1998**, *80*, 2622.
(67) Eaves, J. D.; Tokmakoff, A.; Geissler, P. L. *J. Phys. Chem. A* **2005**, *109*, 9424.
(68) Piryatinski, A.; Lawrence, C. P.; Skinner, J. L. *J. Chem. Phys.* **2003**, *118*, 9664.
(69) Piryatinski, A.; Lawrence, C. P.; Skinner, J. L. *J. Chem. Phys.* **2003**, *118*, 9672.
(70) Weinhold, F.; Landis, C. *Valency and Bonding: A Natural Bond Orbital Donor−Acceptor Perspective*; Cambridge University Press: Cambridge, 2005.
(71) Pimentel, G. C.; McClellan, A. L. *The Hydrogen Bond;* W. H. Freeman and Company: San Francisco, 1960.
(72) Corcelli, S. A.; Lawrence, C. P.; Asbury, J. B.; Steinel, T.; Fayer, M. D.; Skinner, J. L. *J. Chem. Phys.* **2004**, *121*, 8897.